2020 Electrical Insulation Conference (EIC), Virtual Event, June 22 – July 03, 2020

A Review on Dielectric Properties of Supercritical Fluids

Jia Wei
School of Electrical and Computer Engineering
Georgia Institute of Technology
Atlanta, GA, USA
jia.wei@gatech.edu

Alfonso Cruz
School of Electrical and Computer Engineering
Georgia Institute of Technology
Atlanta, GA, USA
acruz@gatech.edu

Chunmeng Xu
School of Electrical and Computer Engineering
Georgia Institute of Technology
Atlanta, GA, USA
chunmengxu@gatech.edu

Farhina Haque
Department of Electrical and Computer Engineering
Mississippi State University
Mississippi State, MS, USA
fh317@msstate.edu

Chanyeop Park
Department of Electrical and Computer Engineering
Mississippi State University
Mississippi State, MS, USA
chanyeop.park@ece.msstate.edu

Lukas Graber
School of Electrical and Computer Engineering
Georgia Institute of Technology
Atlanta, GA, USA
lukas.graber@ece.gatech.edu

***Abstract*— Supercritical fluid (SCF), an intermediate state between gas and liquid, has been recently considered for being used as insulating media owing to properties that show exceptional dielectric strength, high heat transfer capability, and low viscosity. However, research on utilizing SCFs for power applications is still in its early stage, leaving literature and useful data on this topic very limited. This paper reviews and compares available literature related to the dielectric properties of SCFs, especially the electrical breakdown characteristics. Representative researches on the experimental demonstration of the discharge phenomenon in SCFs are summarized in this review. Important transport properties of SCFs, including viscosity, heat capacity, and thermal conductivity, are discussed. Furthermore, key parameters that define their dielectric properties, including conductivity and permittivity, are compared and summarized. Applications that require strong electric fields, efficient heat dissipation, and fast motion can benefit from using SCFs as a dielectric medium. The objective of this study is to provide a new perspective and useful recommendations on the selection of dielectric media for various practical purposes.**

Keywords— supercritical fluids, breakdown, dielectric medium, conductivity, permittivity

I. Introduction

Supercritical fluid (SCF) refers to a state of substance in which the temperature and pressure are above its critical point, where $T \geq T_c$ and $P \geq P_c$. SCFs are widely studied and applied in chemistry, due to favorable properties in diffusivity, solubility, and density. Traditionally, chemical applications of SCFs include extraction of products from natural materials [1, 2], polymer processing [3], and drying [4]. Beyond chemical applications, SCFs have also drawn much attention because of enabling current and emerging applications as heat transfer fluids in concentrating solar power [5], solar water heater [6], and carbon capture and storage [7].

Newer applications include the use of SCFs in combination with electrical discharge. The investigation of electric discharge in SCFs has been a continuing effort for decades, yet most studies are related to the generation of electric plasmas in SCFs for chemical synthesis and nanomaterials fabrication [8, 9]. There are few reports on utilizing SCFs as dielectric media for power applications. As a relatively new field of research, the feasibility of SCFs to replace conventional insulating media has come into public notice [10-12]. However, data specifically about the dielectric and insulating characteristics of SCFs are still scarce. Therefore, the main objective of this review is to compare and summarize available literature related to dielectric properties of SCFs, and present recent progress on the effective characterization methods for evaluating dielectric properties of SCFs.

This review is structured as follows: first, the transport properties of SCFs are introduced subsequently a discussion of the unique characteristics of SCFs that could influence the dielectric property, including density fluctuation, molecular clustering, and cluster size is presented. In the second part, representative studies on the investigation of SCFs with a focus on dielectric properties are summarized. Additionally, electrical testing methods for characterizing dielectric properties of SCFs are discussed. Finally, we demonstrate existing and potentially new applications that could benefit from using SCF as the insulating and dielectric medium.

II. Physical Properties of SCFs

A. Transport Properties

In general, SCF represents the intermediate state of matter between liquid and gaseous states. As an example, Fig. 1 (a) shows a density-pressure (ρ - P) diagram of carbon dioxide

978-1-7281-5485-5/20/$31.00 ©2020 IEEE

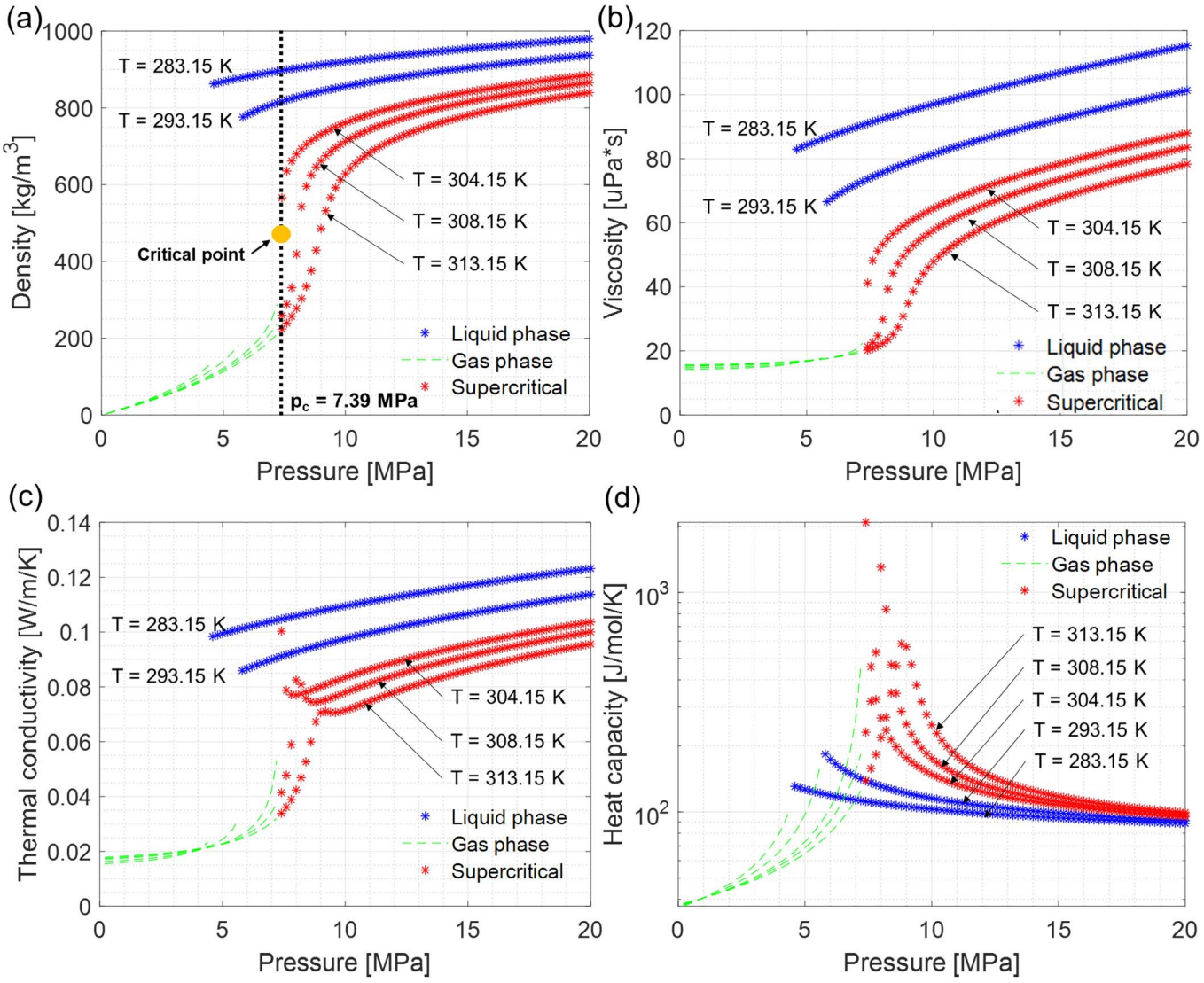

Fig. 1. (a). Density – pressure (ρ - P) diagram of carbon dioxide (CO_2) with isothermal lines. The critical point for CO_2 is represented by the yellow dot at T_c = 304.1 K, P_c = 7.39 MPa [13]. (b). Comparison of the viscosity of CO_2 in three different states. The viscosity of SCFs lies between that of liquids and gases. (c). Comparison of thermal conductivity of CO_2, and (d) compares the heat capacity of CO_2 in gaseous, liquid, and SCF. Green dashed lines represent the fluid in the gaseous phase. Blue and red asterisks represent the fluid in the liquid phase and the supercritical state, respectively [14].

(CO_2) with isothermal lines. The critical point for CO_2 is represented by the yellow dot at T_c = 304.1 K, P_c = 7.39 MPa [13]. Small changes in the CO_2 pressure result in large changes in the density near the critical point. During phase change of CO_2 at a constant pressure below the critical pressure ($P < P_c$), CO_2 transits from liquid to vapor for all temperature values. On the other hand, when CO_2 is at a constant pressure above the critical pressure ($P > P_c$), it can condense into the liquid state by cooling, but it cannot achieve the gaseous phase by merely heating the fluid.

Many of the physical properties of SCFs, such as density and viscosity, are between those of liquids and gases, as shown in Fig. 1(a) and Fig. 1 (b). While this is not true for some other properties like thermal conductivity and heat capacity, which are maximized near the critical point, as shown in Fig. 1 (c) and Fig. 1 (d) [14].

B. Unique Structural Characteristics of SCFs

One of the intriguing characteristics of SCFs rests in the anomalous behavior of fluids near the critical point. As mentioned in the previous section, some physical properties like thermal conductivity and heat capacity reach maximum values in the vicinity of the critical point. Similar anomalies have also been reported in the electrical discharge area. For example, the decrease of breakdown voltages for micrometer-scale gap electrodes [15, 16], the local decrease of the plasma temperature [17], and the local maxima of atomic emission intensities generated by pulsed laser ablation plasmas [18, 19] are all observed near the critical point. Such critical anomalies can be further explained and investigated from the microscopic point of view by the molecular clustering, as well as the macroscopic point of view by the density fluctuation.

The formation of clusters greatly influences the transport properties and the structures of SCFs. Comparing with clusters in solids and liquids, clusters in SCFs consist of molecules with relatively weak intermolecular forces such as van der Waals forces. Also, the average cluster lifetime in SCF is much shorter than that in solids and liquids. The cluster size and the number of molecules in an SCF cluster can be calculated from the Ornstein-Zernike correlation length ξ. According to the Ornstein-Zernike theory, the correlation length ξ can be determined from the characterization of the material using Small Angle X-ray Scattering (SAXS) [20]:

$$I(s) = \frac{I(0)}{1 + \xi^2 s^2} \tag{1}$$

where $I(s)$ is the scattering intensity, and $I(0)$ is the zero-angle scattering intensity at $s = 0$. s is a measure of the scattering angle defined as:

$$s = \frac{4\pi \sin\theta}{\lambda} \tag{2}$$

where θ is the scattering angle, and λ is the x-ray source wavelength.

Data obtained from the SAXS experiment are also related to density fluctuation F_D, which quantifies the extent of the molecular clustering [20]:

$$F_D = \frac{\langle (N - \langle N \rangle)^2 \rangle}{\langle N \rangle} = \frac{I(0)}{N}\frac{1}{Z^2} = \frac{(n_s V)^2}{n_{ave} V} = \frac{k_T}{k_T^0} \tag{3}$$

where N is the total number of particles in a given volume V, $\langle N \rangle$ is the average of N, Z is the number of electrons in a molecule, n_s is the standard deviation of the local number density, n_{ave} is the average number density, k_T is the isothermal compressibility, and k_T^0 is the value of k_T for an ideal gas. Fig. 2 (a) schematically illustrates a fluid with negligible molecular clustering and density fluctuation. Fig. 2 (b) represents a fluid under the condition where the density fluctuation F_D is large.

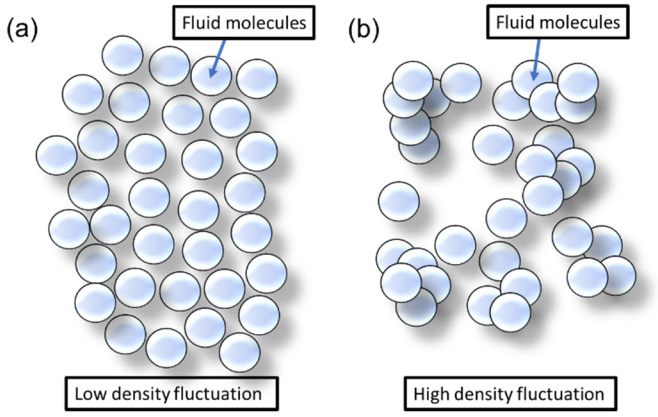

Fig. 2. Schematics of (a) the fluid with molecules with low density fluctuation F_D value, and (b) the fluid with molecules under the condition where the formation of clusters and the density enhancement are substantial, thus the fluid has a high density fluctuation F_D value.

III. Dielectric Properties of SCFs

Experimental investigations on the dielectric property of SCFs always require the testing apparatus to have the capabilities to endure high temperature and high pressure while maintaining sufficient sealing capabilities. Stainless steel has been commonly chosen as the material of the main body. If measurements involving the optical method is required, such as SAXS or laser schlieren, optically transparent materials including sapphire [21], diamond [22], quartz [23], beryllium (Be) [24], and zinc selenide (ZnSe) [25] have been used as the observing window on the testing apparatus.

A. Electrical breakdown characteristics

The electrical breakdown characteristics of SCFs have been investigated under different conditions and methods, as summarized in Table 1. The discharge phenomenon in SCFs has usually been compared with the established theory of gas discharge known by the work of Townsend [26] and Paschen [27]. The gas discharge theory illustrates that under a uniform electric field, the breakdown voltage V_{bd} can be expressed as [27]:

$$V_{bd} = \frac{BPd}{\ln\left[\frac{APd}{\ln\left(\frac{1}{\gamma}\right)}\right]} \tag{4}$$

where A and B are constants about a specific gas type determined by experiments, γ is the third Townsend ionization coefficient which represents the average of secondary electron emissions per positive ion hitting the cathode, P is the pressure, and d is the electrode gap.

Given that the type of gas and the material of the cathode are determined, and A, B, and γ are known, V_{bd} is only the function of the product of pressure P and gap distance d. However, the theory only applies well at the situation of the discharge test at a low pressure, with a small Pd value. Under the circumstance where the discharge happens in a highly pressurized medium like SCF, especially when the electrode gap distance is below 10 μm, V_{bd} starts to deviate from values estimated from Paschen's law. Particularly, in the vicinity of the critical point, this breakdown anomaly is more notable by showing a local decrease in breakdown voltage. Such breakdown anomaly near the critical point has been found and reported by Ito *et al*. under the DC discharge in supercritical CO_2, with gap distances d of 1 μm and 10 μm [15, 16]. Similarly, Sawada *et al*. conducted experiments on supercritical H_2O and Xe and found the anomalous breakdown behavior near the critical point with a coplanar film electrode setup in a 1 μm gap [28]. Supercritical He has also been reported to exhibit such breakdown anomaly by Muneoka *et al.* [29] with tungsten electrodes separated by a 3 μm gap. The formation of molecular clusters can explain this breakdown anomaly, given the increased electron mean free paths near the critical point. In a supercritical state, the microscopic structure of the fluid is characterized by inhomogeneity in the molecular distribution due to the distinct clusters of molecules. Especially, under the conditions close to the critical point, the density fluctuation F_D increases substantially due to constant aggregation and dispersion of clusters, which affects the breakdown strength significantly.

TABLE 1. REPRESENTATIVE RESEARCHES ON THE EXPERIMENTAL DEMONSTRATION OF THE ELECTRICAL BREAKDOWN CHARACTERISTICS OF SCFS

Investigator	Year	Test medium	Experimental demonstration			
			Experimental condition (P, T, ρ)	Experimental method	Electrode and gap distance (d)	Measured breakdown voltage / field (V_{bd} / E_{bd})
Furusato *et al.* [17]	2018	CO_2	ρ = 27.9 - 613.7 kg/m^3 T = 306 K	Pulsed voltage rising rate = 0.7 kV/ns	Point-to-plane d = 1 mm	V_{bd} = 30 - 60 kV
Abid *et al.* [30]	2018	N_2	P = 0.1 - 9.8 MPa	DC	Sphere-to-sphere 10 mm diameter, d = 20 mm	V_{bd} = 60 - 450 V
Seeger *et al.* [31]	2017	Synthetic air, CO_2, CO_2/O_2 mixture, and CF_4	P = 0.5 - 10 MPa	Impulse	d = 5 mm	$E_{air\_saturate}$ = 26 - 30 kV/mm $E_{CO2\_saturate}$ = 22 - 30 kV/mm $E_{CO2/O2\_saturate}$ = 40 kV/mm $E_{CF4\_saturate}$ = 20 - 30 kV/mm
Zhang *et al.* [12]	2015	N_2	P = 1 - 4 MPa	Impulse with 2 kV/ns, 2.5 kV/μs, and 1.66 kV/ms	d = 0 – 1.2 mm	E_{bd_max} = 180 kV/mm
Zhang *et al.* [32]	2014	N_2	P = 1 - 8 MPa T = 300 K	Impulse No flow and slight flow	d = 0.18 – 0.5 mm	V_{BD} = 70 kV
Yang *et al.* [11]	2014	CO_2	T = 305, 298, 293 K P = 7.5, 6 MPa	Pulsed voltage rising rate = 0.75 kV/ns	Sphere-to-sphere 10 mm radius, d = 50 μm	V_{max} = 16 kV
Pai *et al*. [33]	2014	CO_2	P = 0.1 - 7.9 MPa T = 304.3 K	10 kHz AC	Surface dielectric barrier discharges setup, borosilicate glass thickness = 50 μm	$V_{saturate}$ = 2.5 kV
Ihara *et al.* [34]	2012	CO_2	P = 0.1 - 12 MPa T = 298, 305 K	Impulse	Needle-to-plane, tip radius = 5 μm d = 5 mm	V_{bd_max} = 30 kV
Ihara *et al.* [21]	2011	CO_2	P = 7.8 MPa T = 305 K	Impulse	Needle-to-plane, tip radius = 5 μm d = 7 mm	V_{bd} = 65 kV / E_{bd} = 9 kV/mm
Kiyan *et al.* [35]	2011	CO_2	T = 313 K ρ = 50 - 600 kg/m^3	DC	Spherical with diameter of 5 mm and 20 mm; cone-to-cone 1 mm diameter tip d = 140 μm	V_{bd_max} = 55 kV
Kiyan *et al.* [36]	2007	CO_2	P = 0.1 - 14 MPa T = 298, 305, 313 K	DC	Point-to-plane, tip radius = 35 μm d = 200 μm	V_{bd_max} = 35 kV
Sawada *et al*. [28]	2006	H_2O and Xe	P_{H2O} = 0.1 - 28 MPa T_{H2O} = 650.65 K P_{Xe} = 0.1 - 8 MPa T_{Xe} = 292.15 K	DC	Plane-to-plane (coplanar film electrodes) d = 1 μm	V_{H2O_max} = 2.5 kV V_{Xe_max} = 0.8 kV
Lock *et al.* [23, 37]	2005	CO_2	P = 8 MPa T = 310 K	DC	Point-to-plane and wire-to-plane d = 110 μm	V_{bd} = 18 kV
Ito *et al.* [15, 16]	2002	CO_2	P = 0.1 - 10 MPa T = 305.65, 308.15, 313.15 K	DC	Plane-to-plane (coplanar film electrodes) d = 1, 10 μm	V_{bd} = 500 V

B. *Conductivity and permittivity*

Electrical conductivity σ quantifies how strongly the material conducts electric current. It is defined as the ratio of the density of the current to the electric field [38]:

$$\sigma = \frac{J}{E} \tag{5}$$

where J is the current density, and E is the electric field. In the case that the SCF is considered as the dielectric medium, positive and negative ions are the main current carriers. The current density is determined by the formula [39]:

$$J = qnv_a \tag{6}$$

where q is the charge of carriers, n is the density of charge carriers, and v_a is the average speed of the charge carrier's movement.

There are few reports on the electrical conductivity of SCFs available in the literature. In general, the values of the electrical conductivity σ of SCFs are very low. Hefner *et al*. conducted the electrical conductivity measurement of supercritical mercury (Hg), and σ values are below 10^{-1} S/m [40]. Like the anomalous behavior observed in the electrical breakdown, the electrical conductivity also exhibits such critical anomaly near the critical point. Hoshino *et al*. found the electrical conductivity of selenium (Se) drops sharply toward more insulating behavior in supercritical state [41].

Another important parameter that helps to understand the dielectric properties of SCFs is the complex permittivity ε, which represents the material's ability to respond to the electric field by its polarization. The complex permittivity ε has the real component ε' and the imaginary component ε'' such that:

$$\varepsilon = \varepsilon' - j\varepsilon'' \tag{7}$$

where the real part ε' quantifies the charge storage capacity, and the imaginary part ε'' attributes to bound charge and dipole relaxation phenomena.

Studies on the permittivity of SCFs are also very scarce. Testemale *et al*. observed that the permittivity of water shows a decrease as getting closer to the critical point [42]. Skaf *et al*. performed a theoretical analysis of the permittivity of supercritical water. Their result shows the highest relative permittivity of 16.3 at 650 K [43].

IV. Applications of SCFs as Dielectric Media

Besides applications mentioned in the introduction, many applications that require strong electric fields, efficient heat dissipation, and fast motion could benefit from such a new dielectric fluid. Three potential applications that can be made more feasible, efficient, and cost-effective are discussed in this section.

A. *Ultra-fast switchgear*

Ultra-fast switchgear provides opportunities for DC circuit breakers, which enable the use of meshed DC power systems such as those required for power distribution on all-electric ships and electric aircraft [44] as well as multi-terminal high voltage DC power transmission [45]. Transcontinental exchange of renewable energy can eventually be achievable by enabling the new design of DC circuit breakers with supercritical fluids as dielectric media. Non-arcing disconnect switches with a new operating mechanism such as piezoelectric actuators also can be integrated with a new type of insulating medium for enhanced performances [46, 47]. Supercritical fluids as new dielectric media with high dielectric strength and low viscosity allow reducing the contact travel, therefore allowing much faster switching operation. Fig.3 shows the schematic diagram of two potential applications: a high speed disconnect switch (Fig. 3 (a)), and a circuit breaker (Fig. 3 (b)).

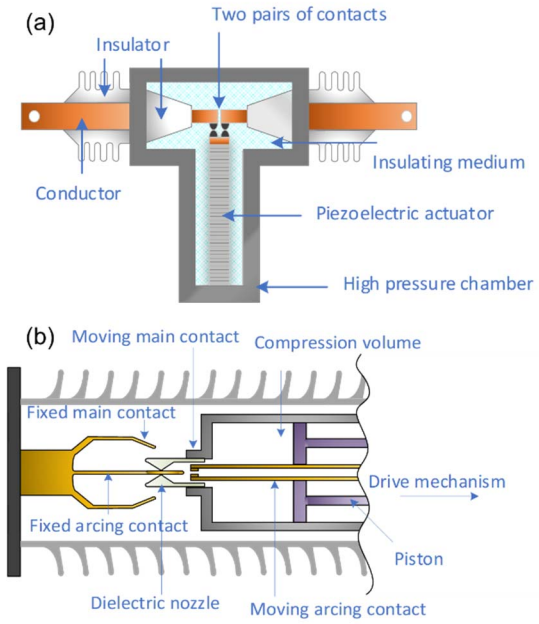

Fig. 3. Conceptual drawings of applications for ultra-fast switchgear that could benefit from using SCFs as dielectric media: (a) the high speed disconnect switch, and (b) the circuit breaker.

B. *Electrostatic rotating machines*

For certain applications, electrostatic machines are preferred over electromagnetic machines due to their relatively simple structures, manufacturability, and higher power density. Ge *et al.* investigated and compared ultra-high vacuum, dielectric gas, and liquid dielectrics for electrostatic motors. Ultra-high vacuum and gaseous dielectrics can only provide limited torque, and the machines have to spin at a very high speed to develop power. Viscosity is the main issue for liquids since it determines the drag losses which influence the speed range of the machine [48, 49]. A dielectric medium which combines high dielectric strength as well as low viscosity is ideal for this application. Fig. 4 shows a schematic diagram of an electrostatic motor.

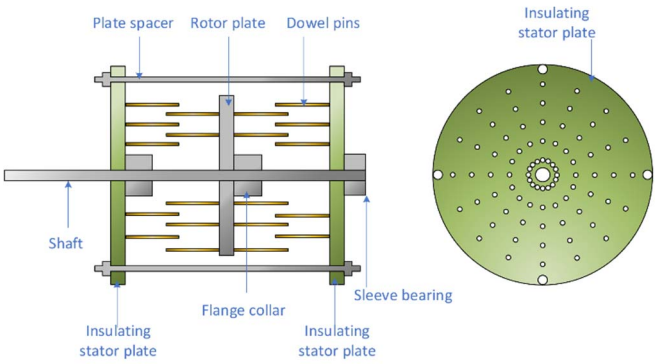

Fig. 4. A prototype electrostatic machine built by Ge *et al.* [48]. Such a machine can achieve a higher force because the voltage across micro-scale distances produces strong electric fields. Electrostatic machines would neither require heavy permanent magnets nor iron rotor/stator systems.

C. Van de Graaff generators

Linear accelerators often rely on van de Graaff generators to provide ultra-low ripple DC voltage to supply ions. The limited dielectric strength of the insulation gas in which the generators operate increases the size of the installation. SCFs could shrink the size of such accelerators, reducing their cost, and ultimately allow more widespread use. The use of SCFs would benefit high energy research as well as medical applications [50, 51]. Fig. 5 shows a van de Graaff generators in a linear particle accelerator.

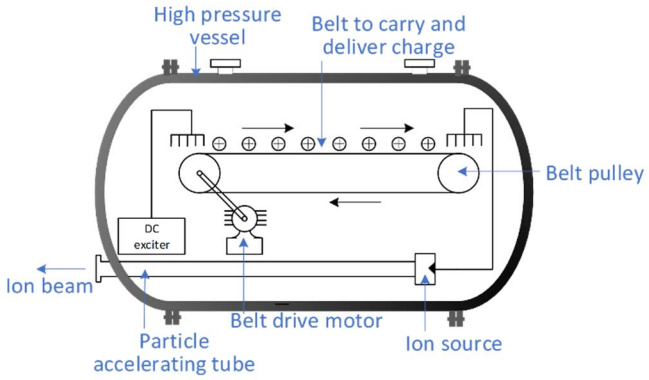

Fig. 5. Schematic diagram for a tandem Van de Graaff generator in a linear particle accelerator. Using SCFs as insulating media enables a more compact design so that it can be widely adopted.

V. Conclusion

In this review, we have given a summary of available literature related to the investigation of the dielectric properties of SCFs. Specifically, we have focused on the purpose of using SCFs as a dielectric medium. Transport properties, including density, viscosity, thermal conductivity, and heat capacity of CO_2, have been compared in three different states. We have also discussed the unique characteristics of SCFs, such as density fluctuation and molecular clustering, which influence the dielectric property. Experimental results on the electric discharge behavior of SCFs have been compared and summarized with an emphasis on breakdown phenomena. We have also presented existing technologies that could benefit from such a new dielectric medium due to the need for strong electric fields, efficient heat dissipation, and fast motion. As traditional insulating and dielectric media all have nonnegligible disadvantages in applications, we hope this paper could provide a new perspective on the selection of dielectric media for various practical purposes. We also expect more studies on the subject of using SCFs as dielectric media, especially the investigation on the conductivity, permittivity, and dielectric loss of SCFs, to be carried out soon in the future.

References

[1] M. McHugh and V. Krukonis, *Supercritical fluid extraction: principles and practice*. Elsevier, 2013.

[2] Ž. Knez, E. Markočič, M. Leitgeb, M. Primožič, M. K. Hrnčič, and M. Škerget, "Industrial applications of supercritical fluids: A review," *Energy,* vol. 77, pp. 235-243, 2014.

[3] C. A. Eckert, B. L. Knutson, and P. G. Debenedetti, "Supercritical fluids as solvents for chemical and materials processing," *Nature,* vol. 383, no. 6598, p. 313, 1996.

[4] S. P. Sawan and S. P. Sawan, *Supercritical fluid cleaning: fundamentals, technology and applications*. Elsevier, 1998.

[5] J. I. Linares, L. E. Herranz, I. Fernández, A. Cantizano, and B. Y. Moratilla, "Supercritical CO2 Brayton power cycles for DEMO fusion reactor based on Helium Cooled Lithium Lead blanket," *Applied Thermal Engineering,* vol. 76, pp. 123-133, 2015.

[6] H. Yamaguchi, N. Sawada, H. Suzuki, H. Ueda, and X. Zhang, "Preliminary study on a solar water heater using supercritical carbon dioxide as working fluid," *Journal of Solar Energy Engineering,* vol. 132, no. 1, p. 011010, 2010.

[7] F. Luo, R.-N. Xu, and P.-X. Jiang, "Numerical investigation of fluid flow and heat transfer in a doublet enhanced geothermal system with CO2 as the working fluid (CO2–EGS)," *Energy,* vol. 64, pp. 307-322, 2014.

[8] S. Stauss, H. Muneoka, K. Urabe, and K. Terashima, "Review of electric discharge microplasmas generated in highly fluctuating fluids: characteristics and application to nanomaterials synthesis," *Physics of Plasmas,* vol. 22, no. 5, p. 057103, 2015.

[9] H. Muneoka, K. Urabe, S. Stauss, and K. Terashima, "Micrometer-scale electrical breakdown in high-density fluids with large density fluctuations: Numerical model and experimental assessment," *Physical Review E,* vol. 91, no. 4, p. 042316, 2015.

[10] Y. Tian, J. Wei, C. Park, Z. Wang, and L. Graber, "Modelling of electrical breakdown in supercritical CO 2 with molecular clusters formation," in *2018 12th International Conference on the Properties and Applications of Dielectric Materials (ICPADM)*, 2018: IEEE, pp. 992-995.

[11] Z. Yang, S. Hosseini, T. Kiyan, S. Gnapowski, and H. Akiyama, "Post-breakdown dielectric recovery characteristics of high-pressure liquid CO 2 including supercritical phase," *IEEE Transactions on Dielectrics and Electrical Insulation,* vol. 21, no. 3, pp. 1089-1094, 2014.

[12] J. Zhang *et al.*, "Breakdown strength and dielectric recovery in a high pressure supercritical nitrogen switch," *IEEE Transactions on Dielectrics and Electrical Insulation,* vol. 22, no. 4, pp. 1823-1832, 2015.

[13] Y. Suehiro, M. Nakajima, K. Yamada, and M. Uematsu, "Critical parameters of {xCO2+ (1− x) CHF3} forx=(1.0000, 0.7496, 0.5013, and 0.2522)," *The Journal of Chemical Thermodynamics,* vol. 28, no. 10, pp. 1153-1164, 1996.

[14] E. Lemmon, M. McLinden, D. Friend, P. Linstrom, and W. Mallard, "NIST chemistry WebBook, Nist standard reference database number 69," *National Institute of Standards and Technology, Gaithersburg,* 2011.

[15] T. Ito and K. Terashima, "Generation of micrometer-scale discharge in a supercritical fluid environment," *Applied physics letters,* vol. 80, no. 16, pp. 2854-2856, 2002.

[16] T. Ito, H. Fujiwara, and K. Terashima, "Decrease of breakdown voltages for micrometer-scale gap electrodes for carbon dioxide near

the critical point: Temperature and pressure dependences," *Journal of applied physics,* vol. 94, no. 8, pp. 5411-5413, 2003.
[17] T. Furusato *et al.*, "Anomalous plasma temperature at supercritical phase of pressurized CO 2 after pulsed breakdown followed by large short-circuit current," *IEEE Transactions on Dielectrics and Electrical Insulation,* vol. 25, no. 5, pp. 1807-1813, 2018.
[18] T. Kato *et al.*, "Pulsed laser ablation plasmas generated in CO2 under high-pressure conditions up to supercritical fluid," *Applied Physics Letters,* vol. 101, no. 22, p. 224103, 2012.
[19] K.-i. Saitow and T. Yamamura, "Effective cooling generates efficient emission: blue, green, and red light-emitting Si nanocrystals," *The Journal of Physical Chemistry C,* vol. 113, no. 19, pp. 8465-8470, 2009.
[20] H. E. Stanley, *Phase transitions and critical phenomena*. Clarendon Press, Oxford, 1971.
[21] T. Ihara, T. Kiyan, S. Katsuki, T. Furusato, M. Hara, and H. Akiyama, "Positive pulsed streamer in supercritical carbon dioxide," *IEEE Transactions on Plasma Science,* vol. 39, no. 11, pp. 2650-2651, 2011.
[22] T. Morita, K. Kusano, H. Ochiai, K.-i. Saitow, and K. Nishikawa, "Study of inhomogeneity of supercritical water by small-angle x-ray scattering," *The Journal of Chemical Physics,* vol. 112, no. 9, pp. 4203-4211, 2000.
[23] E. H. Lock, A. V. Saveliev, and L. A. Kennedy, "Initiation of pulsed corona discharge under supercritical conditions," *IEEE transactions on plasma science,* vol. 33, no. 2, pp. 850-853, 2005.
[24] K. Nishikawa and M. Takematsu, "Construction of sample holder for X-ray diffraction experiments on supercritical fluids," *Japanese journal of applied physics,* vol. 32, no. 11R, p. 5155, 1993.
[25] G. Guevara-Carrion, S. Ancherbak, A. Mialdun, J. Vrabec, and V. Shevtsova, "Diffusion of methane in supercritical carbon dioxide across the Widom line," *Scientific reports,* vol. 9, 2019.
[26] J. S. Townsend, *Electricity in gases*. Рипол Классик, 1915.
[27] F. Paschen, "Ueber die zum Funkenübergang in Luft, Wasserstoff und Kohlensäure bei verschiedenen Drucken erforderliche Potentialdifferenz," *Annalen der Physik,* vol. 273, no. 5, pp. 69-96, 1889.
[28] M. Sawada, T. Tomai, T. Ito, H. Fujiwara, and K. Terashima, "Micrometer-scale discharge in high-pressure H 2 O and Xe environments including supercritical fluid," *Journal of applied physics,* vol. 100, no. 12, p. 123304, 2006.
[29] H. Muneoka, K. Urabe, S. Stauss, and K. Terashima, "Breakdown characteristics of electrical discharges in high-density helium near the critical point," *Applied Physics Express,* vol. 6, no. 8, p. 086201, 2013.
[30] F. Abid, K. Niayesh, E. Jonsson, N. S. Støa-Aanensen, and M. Runde, "Arc voltage characteristics in ultrahigh-pressure nitrogen including supercritical region," *IEEE Transactions on Plasma Science,* vol. 46, no. 1, pp. 187-193, 2018.
[31] M. Seeger, P. Stoller, and A. Garyfallos, "Breakdown fields in synthetic air, CO 2, a CO 2/O 2 mixture, and CF 4 in the pressure range 0.5–10 MPa," *IEEE Transactions on Dielectrics and Electrical Insulation,* vol. 24, no. 3, pp. 1582-1591, 2017.
[32] J. Zhang, B. van Heesch, F. Beckers, T. Huiskamp, and G. Pemen, "Breakdown voltage and recovery rate estimation of a supercritical nitrogen plasma switch," *IEEE Transactions on Plasma Science,* vol. 42, no. 2, pp. 376-383, 2014.
[33] D. Z. Pai, S. Stauss, and K. Terashima, "Surface dielectric barrier discharges exhibiting field emission at high pressures," *Plasma Sources Science and Technology,* vol. 23, no. 2, p. 025019, 2014.
[34] T. Ihara *et al.*, "Initiation mechanism of a positive streamer in pressurized carbon dioxide up to liquid and supercritical phases with nanosecond pulsed voltages," *Journal of Physics D: Applied Physics,* vol. 45, no. 7, p. 075204, 2012.
[35] T. Kiyan, T. Ihara, S. Kameda, T. Furusato, M. Hara, and H. Akiyama, "Weibull statistical analysis of pulsed breakdown voltages in high-pressure carbon dioxide including supercritical phase," *IEEE Transactions on Plasma Science,* vol. 39, no. 8, pp. 1729-1735, 2011.
[36] T. Kiyan *et al.*, "Negative DC prebreakdown phenomena and breakdown-voltage characteristics of pressurized carbon dioxide up to supercritical conditions," *IEEE transactions on plasma science,* vol. 35, no. 3, pp. 656-662, 2007.
[37] E. H. Lock, A. V. Saveliev, and L. A. Kennedy, "Influence of electrode characteristics on DC point-to-plane breakdown in high-pressure gaseous and supercritical carbon dioxide," *IEEE Transactions on Plasma Science,* vol. 37, no. 6, pp. 1078-1083, 2009.
[38] N. Kumar, *Comprehensive physics XII*. Laxmi Publications, 2004.
[39] S. Kasap, C. Koughia, H. Ruda, and R. Johanson, "Electrical conduction in metals and semiconductors," *Springer Handbook of Electronic and Photonic Materials,* pp. 19-45, 2007.
[40] W. Hefner and F. Hensel, "Dielectric anomaly and the vapor-liquid phase transition in mercury," *Physical Review Letters,* vol. 48, no. 15, p. 1026, 1982.
[41] H. Hoshino, R. Schmutzler, W. Warren, and F. Hensel, "The electrical conductivity of fluid selenium up to supercritical temperatures and pressures," *Philosophical Magazine,* vol. 33, no. 2, pp. 255-259, 1976.
[42] D. Testemale *et al.*, "Small angle x-ray scattering of a supercritical electrolyte solution: The effect of density fluctuations on the hydration of ions," *The Journal of chemical physics,* vol. 122, no. 19, p. 194505, 2005.
[43] M. S. Skaf and D. Laria, "Dielectric relaxation of supercritical water: Computer simulations," *The Journal of Chemical Physics,* vol. 113, no. 9, pp. 3499-3502, 2000.
[44] C. M. Franck, "HVDC circuit breakers: A review identifying future research needs," *IEEE Transactions on Power Delivery,* vol. 26, no. 2, pp. 998-1007, 2011.
[45] D. Van Hertem and M. Ghandhari, "Multi-terminal VSC HVDC for the European supergrid: Obstacles," *Renewable and sustainable energy reviews,* vol. 14, no. 9, pp. 3156-3163, 2010.
[46] L. Graber, S. Smith, D. Soto, I. Nowak, J. Owens, and M. Steurer, "A new class of high speed disconnect switch based on piezoelectric actuators," in *2015 IEEE Electric Ship Technologies Symposium (ESTS)*, 2015: IEEE, pp. 312-317.
[47] L. Graber, C. Widener, S. Smith, and M. Steurer, "Ultrafast electromechanical disconnect switch," ed: Google Patents, 2016.
[48] B. Ge and D. C. Ludois, "Design concepts for a fluid-filled three-phase axial-peg-style electrostatic rotating machine utilizing variable elastance," *IEEE Transactions on Industry Applications,* vol. 52, no. 3, pp. 2156-2166, 2016.
[49] B. Ge and D. C. Ludois, "Dielectric liquids for enhanced field force in macro scale direct drive electrostatic actuators and rotating machinery," *IEEE Transactions on Dielectrics and Electrical Insulation,* vol. 23, no. 4, pp. 1924-1934, 2016.
[50] M. Belli *et al.*, "Proton irradiation facility for radiobiological studies at a 7 MV Van de Graaff accelerator," *Nuclear Instruments and Methods in Physics Research Section A: Accelerators, Spectrometers, Detectors and Associated Equipment,* vol. 256, no. 3, pp. 576-580, 1987.
[51] R. Hellborg, *Electrostatic accelerators*. Springer, 2005.